Institute of Cosmophysical Research
and Radio Wave Propagation FEB RAS
Acoustic Research Laboratory

Overview of processing and analysis methods for pulse geophysical signals

O. Lukovenkova, Yu. Senkevich,
A. Solodchuk, A. Shcherbina

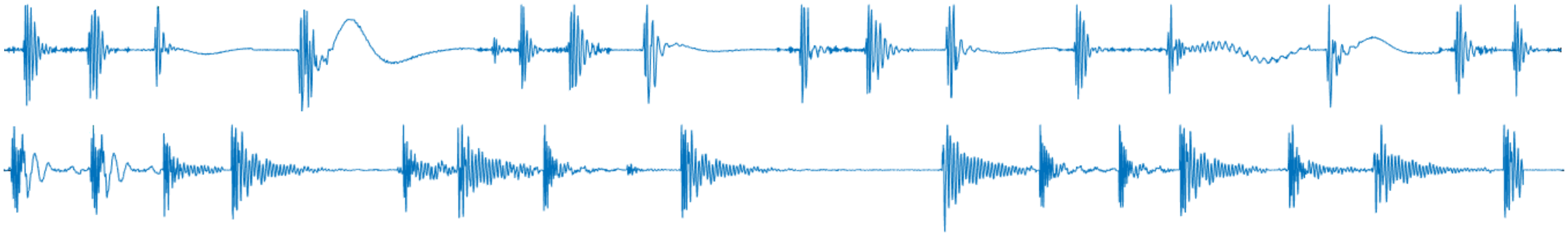

1. Signal model

$$x(t) = \sum_i A_i \cdot g_i(t - \tau_i) + \varepsilon(t)$$

A_i is the amplitude of *i*-th pulse;
$g_i(t)$ is the function describing *i*-th pulse;
τ_i is the generation time of the *i*-th pulse;
$\varepsilon(t)$ is the noise.

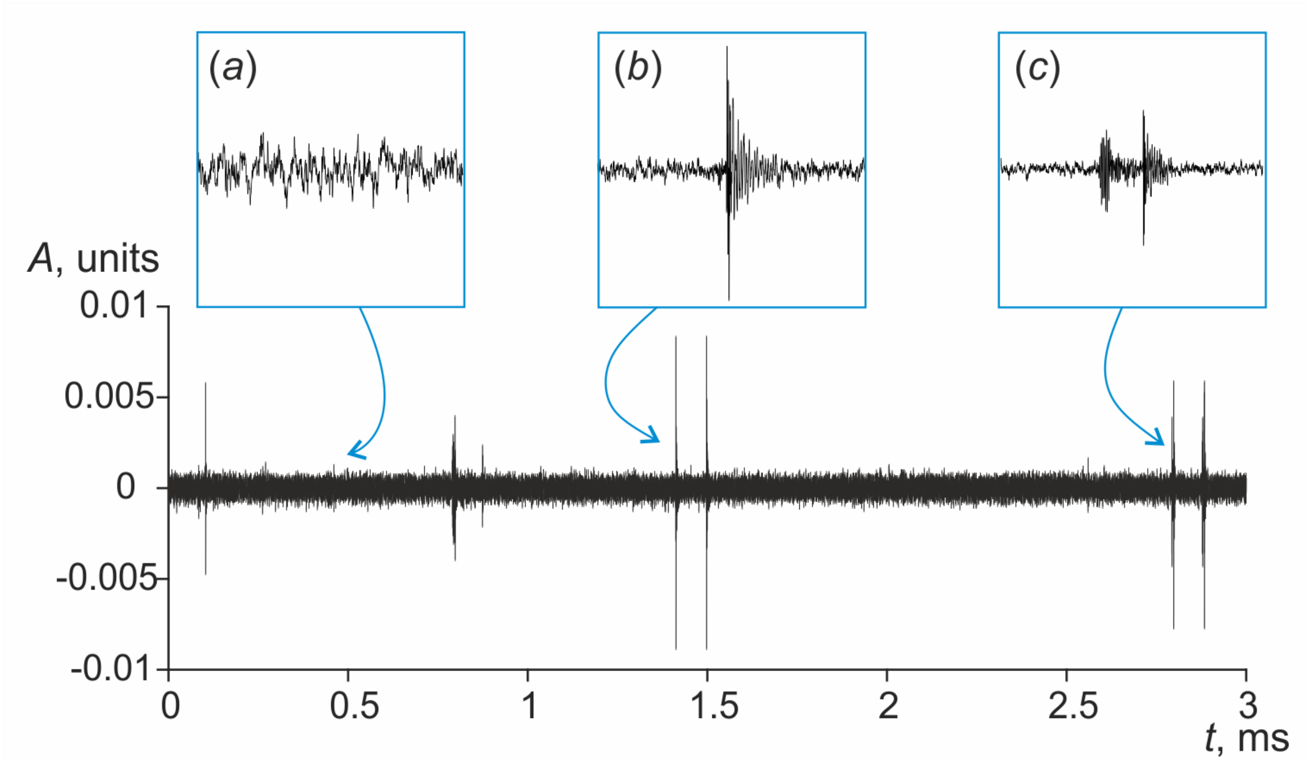

Fig. 1. Geoacoustic emission signal fragment: (*a*) – noise; (*b*), (*c*) – pulses.

2. Waveform reconstruction

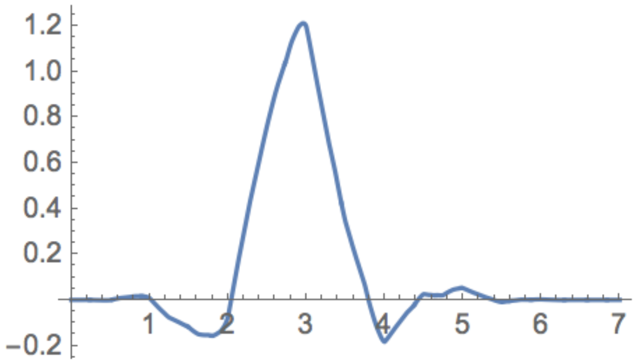

Fig. 2. Sym4 wavelet.

Wavelet denoising:

1) Decomposition

2) Detail coefficients thresholding
(Empirical Bayes method, posterior median rule)

3) *Reconstruction*

2. Waveform reconstruction

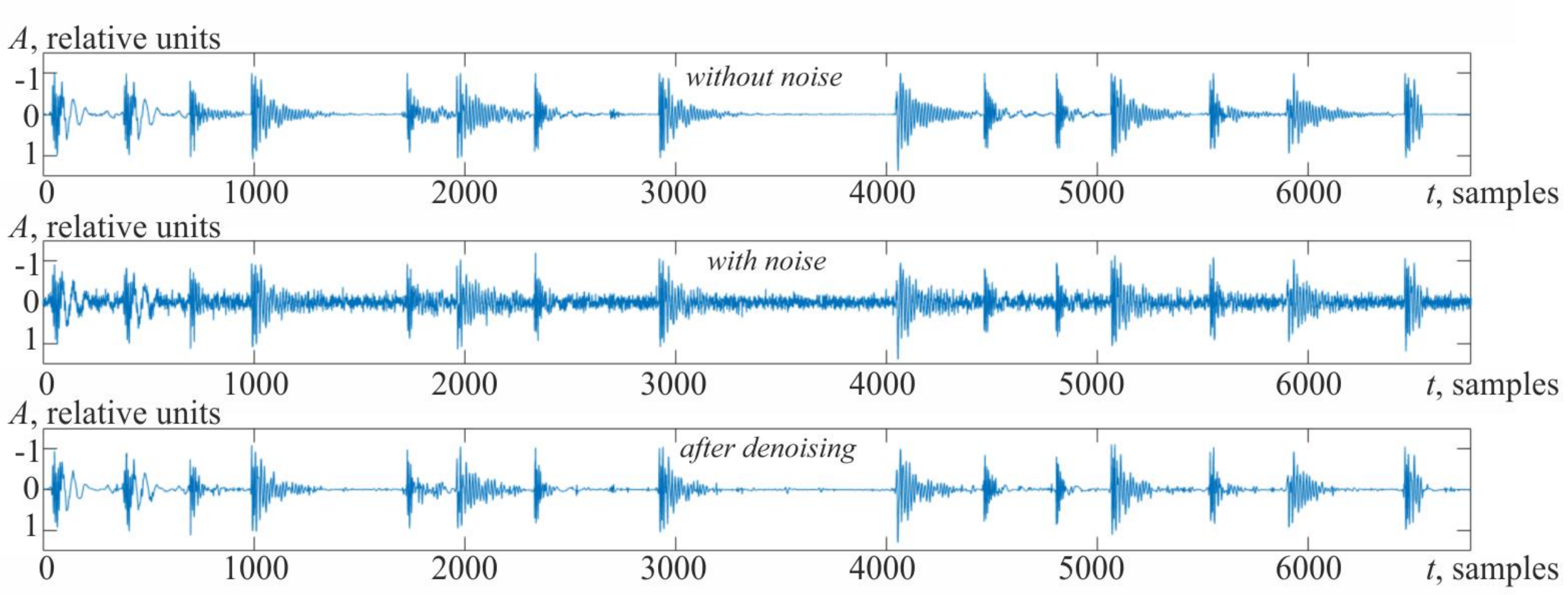

Fig. 3. Waveform reconstruction of noisy geoacoustic signal.

2. Waveform reconstruction

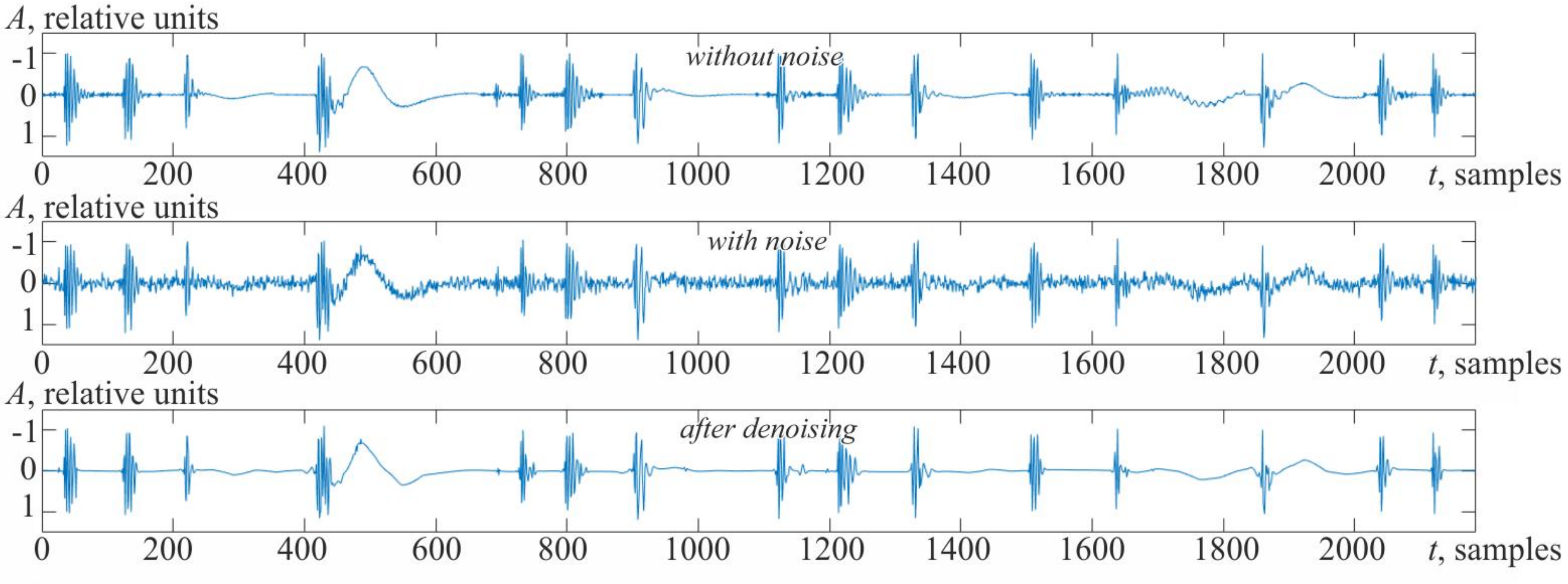

Fig. 4. Waveform reconstruction of noisy electromagnetic signal.

3. Pulse detector

Adaptive threshold

$$S_k = \overline{M_{k-1}} + B \cdot \sigma_{k-1}$$

depends on the background signal level

$\overline{M_{k-1}}$ and σ_{k-1} are the mean value and standard deviation of the previous n samples (n from 200 to 400 samples);

B is the experimentally determined parameter (B from 2.1 to 2.5).

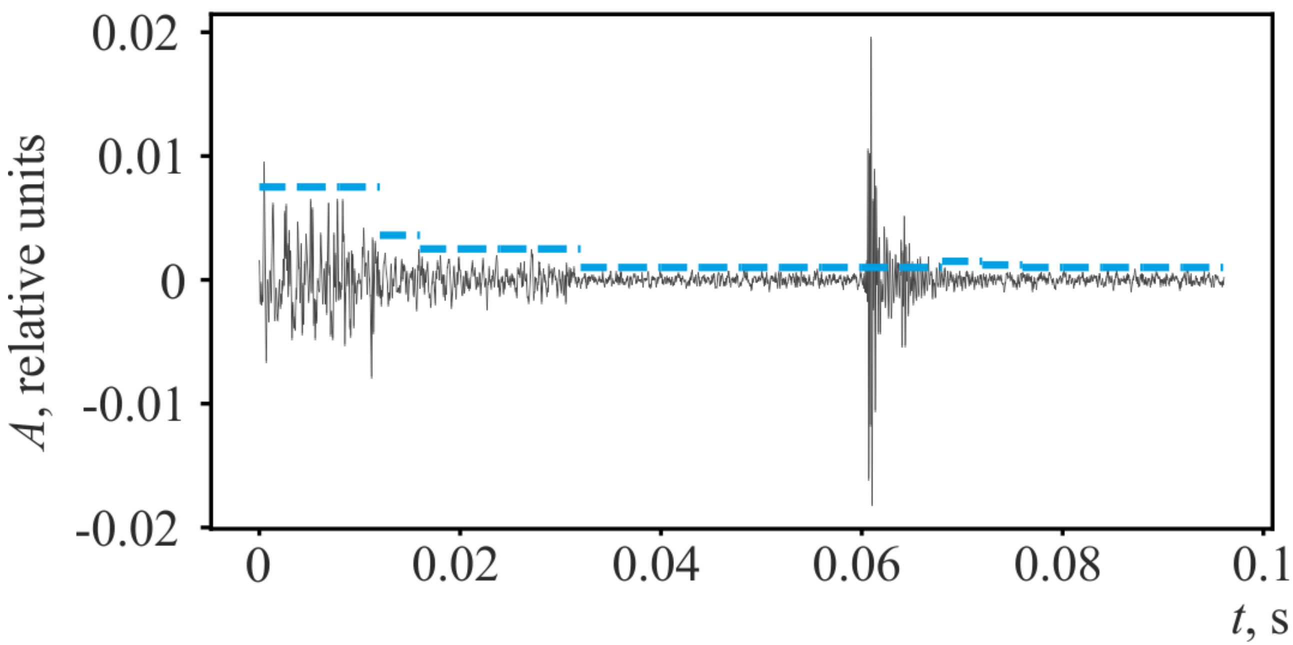

Fig. 5. Geoacoustic emission signal. The dotted line indicates the adaptive pulse detection threshold.

3. Pulse detector

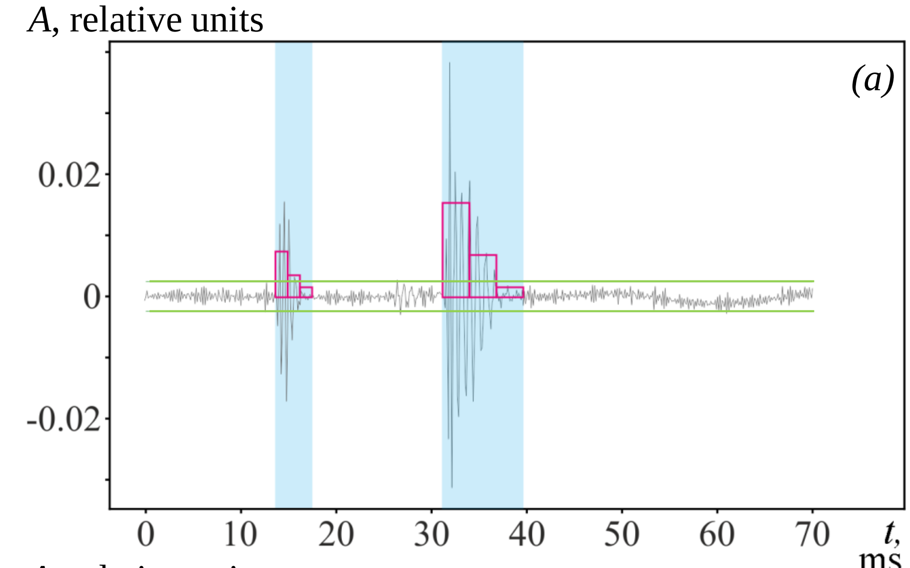

Pulses:

- minimum duration is 0.1 μs;
- $\frac{A_{max}}{S_k} \geq 1.8$;
- additional waveform check**:** the average amplitude of one part exceeds the other ones by more than 1.2 times.

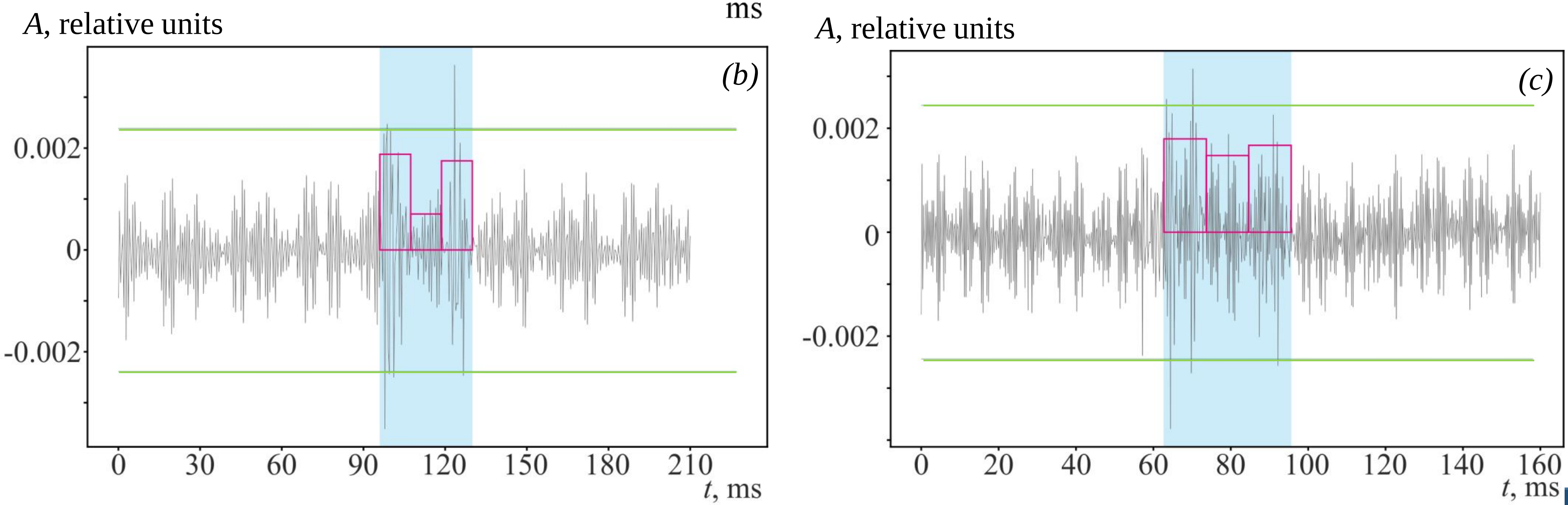

Fig. 6. Examples of detected signal fragments: (*a*) - pulses; (*b*), (*c*) - not pulses.

4. Time-frequency structure analysis

Sparse approximation problem

compact signal representations
without losing accuracy

$$\begin{cases} s(t) = \sum_{m=0}^{N-1} a_m g_m(t), \\ \|a\|_0 \to min. \end{cases}$$

$\|\cdot\|_0$ is the pseudo-norm (L_0-norm) that is equal to the number of nonzero elements of the coefficient vector.

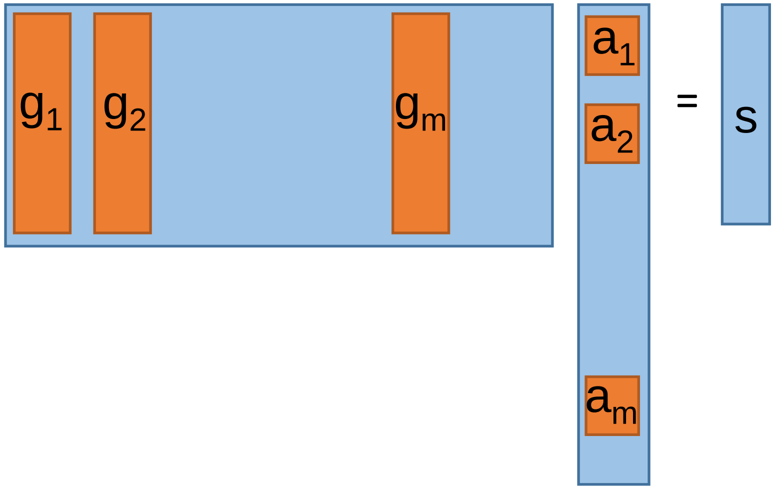

Adaptive Matching Pursuit

$$\begin{cases} s(t) = \sum_{m=0}^{N-1} a_m g_m(t) + R_N, \\ \|R_N\| \to min, \\ \|a\|_0 \le \varepsilon. \end{cases}$$

+

procedure for setting the parameters of the basis function g_m that has the greatest correlation with the signal

$s(t)$ is the signal;
$g_m(t)$ are the basis functions;
a_m are the coefficients of decomposition;
N is the number of components;
R_N is the residual;
ε is the L_0-norm limit.

4. Time-frequency structure analysis

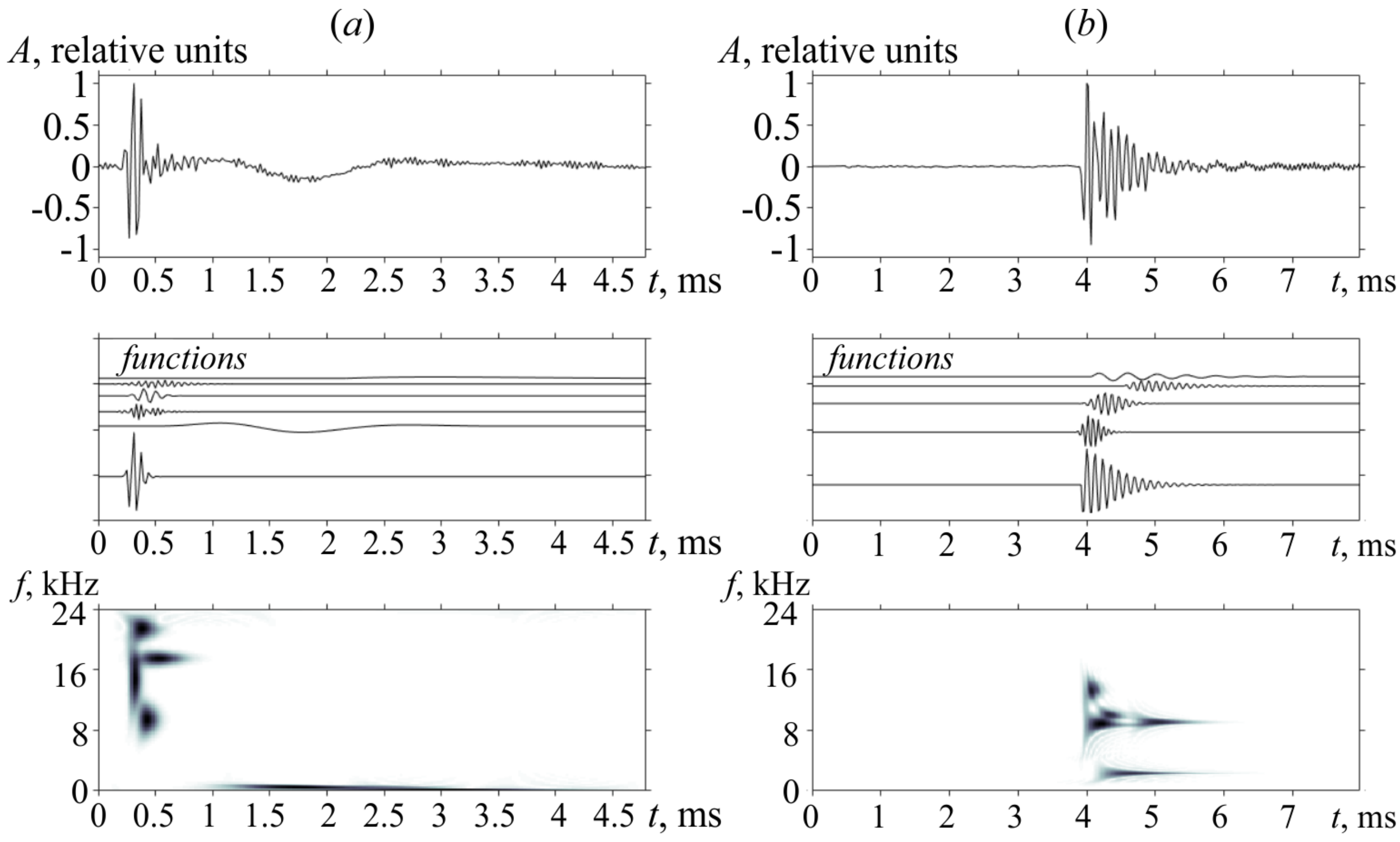

Fig. 7. Time-frequency structure of electromagnetic (*a*) and geoacoustic (*b*) pulses. Gauss and Berlage functions were used.

5. Waveform analysis

Structural description method

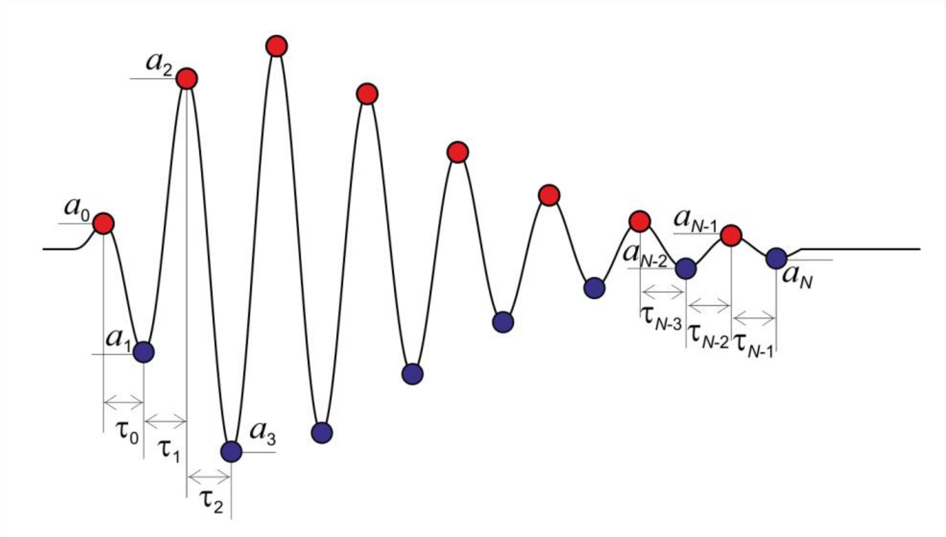

Fig. 8. Pulse local extrema.

Descriptive matrix

$$\mathbf{D} = \begin{pmatrix} r_{0,1} & r_{0,2} & \cdots & r_{0,N-1} & r_{0,N} \\ \omega_{0,1} & r_{1,2} & \cdots & r_{1,N-1} & r_{1,N} \\ \omega_{0,2} & \omega_{1,2} & \cdots & r_{2,N-1} & r_{2,N} \\ \vdots & \vdots & \ddots & \vdots & \vdots \\ \omega_{0,N-2} & \omega_{1,N-2} & \cdots & r_{N-2,N-1} & r_{N-2,N} \\ \omega_{0,N-1} & \omega_{1,N-1} & \cdots & \omega_{N-2,N-1} & r_{N-1,N} \end{pmatrix}$$

$$r_{i,j} = \begin{cases} 1, & a_i > a_j \\ 0, & a_i \le a_j \end{cases}, \qquad \omega_{i,j} = \begin{cases} 1, & \tau_i > \tau_j \\ 0, & \tau_i \le \tau_j \end{cases},$$

$r_{i,j}$ is the result of comparison of the *i*-th and *j*-th extreme amplitudes; $\omega_{i,j}$ is the result of comparison of the *i*-th and *j*-th intervals between the extrema

5. Waveform analysis

(*a*)

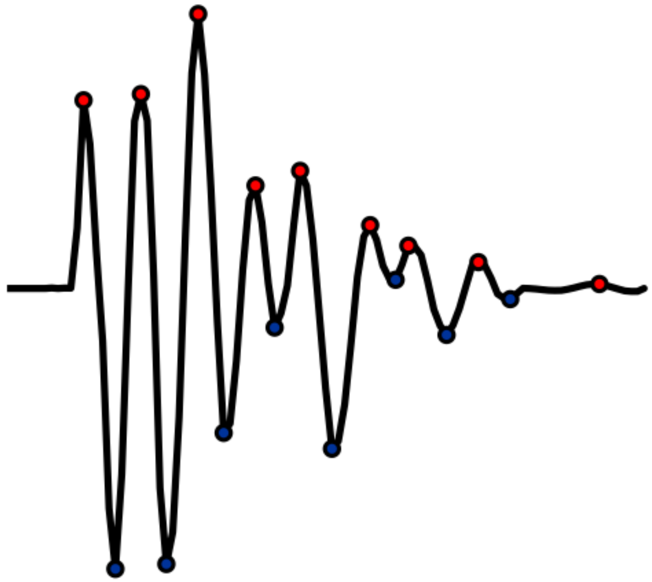

(*b*)

1	0	1	0	1	1	1	1	1	1	1	1	1	1	1	1
1	0	0	0	0	0	0	0	0	0	0	0	0	0	0	0
1	0	1	0	1	1	1	1	1	1	1	1	1	1	1	1
0	0	0	0	0	0	0	0	0	0	0	0	0	0	0	0
1	0	0	1	1	1	1	1	1	1	1	1	1	1	1	1
0	0	0	0	0	0	0	0	1	0	0	0	0	0	0	0
1	1	1	1	1	1	1	0	1	1	1	1	1	1	1	1
1	0	0	1	0	1	0	0	1	0	0	0	1	0	0	0
0	0	0	0	0	0	0	0	1	1	1	1	1	1	1	1
0	0	0	0	0	0	0	0	0	0	0	0	0	0	0	0
1	0	0	1	0	1	0	0	1	1	1	1	1	1	1	1
1	1	1	1	1	1	1	1	1	1	1	0	1	0	1	1
0	0	0	0	0	0	0	0	0	0	0	0	1	1	1	1
0	0	0	0	0	0	0	0	0	1	0	0	1	0	0	0
0	0	0	0	0	0	0	0	0	1	0	0	1	0	1	1
0	0	0	0	0	0	0	0	0	0	0	0	0	0	0	0

Fig. 9. Representation of a pulse by descriptive matrix: (*a*) – pulse with detected extrema; (*b*) – its descriptive matrix.

5. Waveform analysis

Pulse classification

Similarity coefficient g

$$g(\mathbf{D}_1^{(Z)}, \mathbf{D}_2^{(Z)}) = \frac{\#(d_{1ij} = d_{2ij})}{Z^2} > G_0,$$

Z is the matrix order;
G_0 is the empirical threshold.

Possibility for absorption

$$N_L / N_M \geq S_0, \quad 0 < S_0 \leq 1,$$

N_L is smaller matrix order;
N_M is larger matrix order;
S_0 is the empirical threshold.

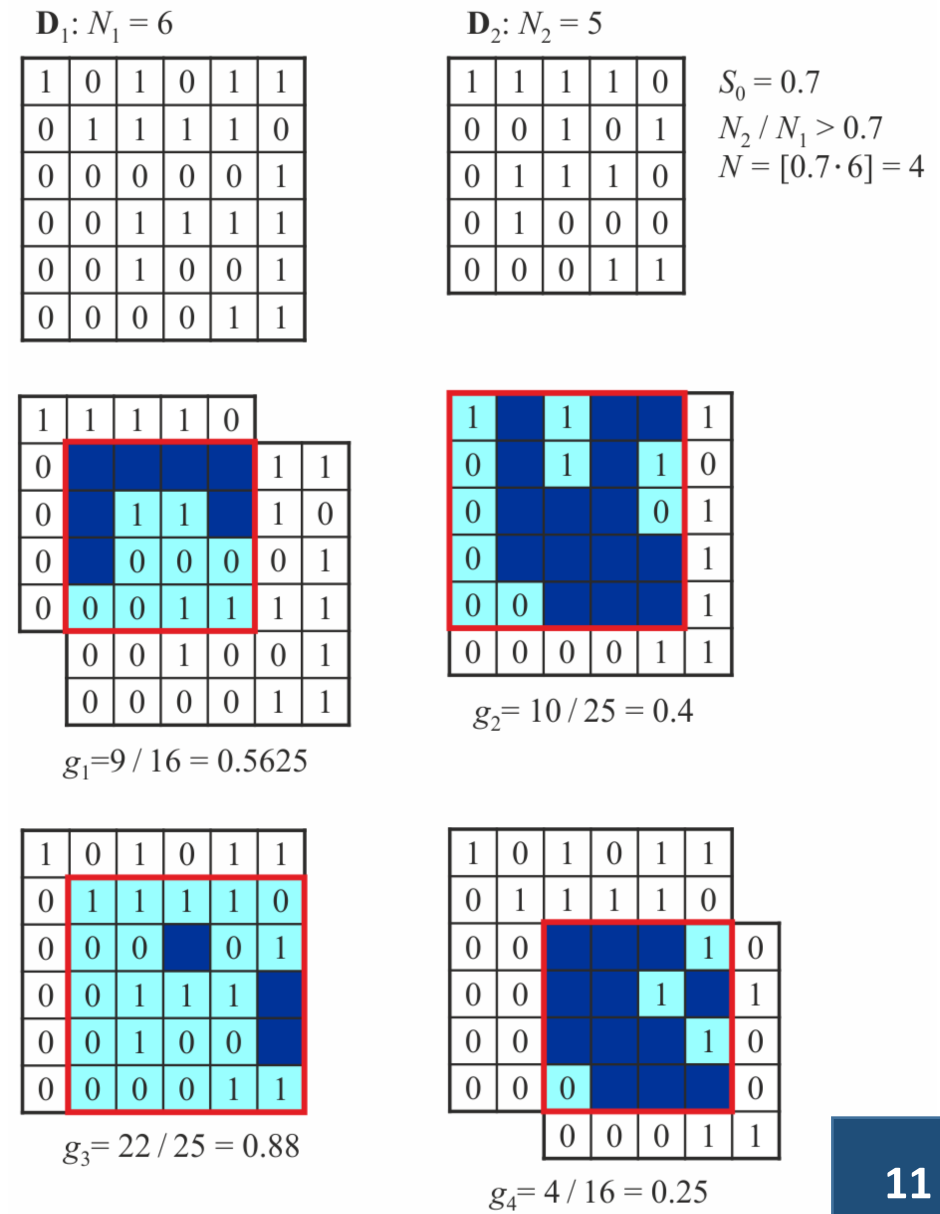

5. Waveform analysis

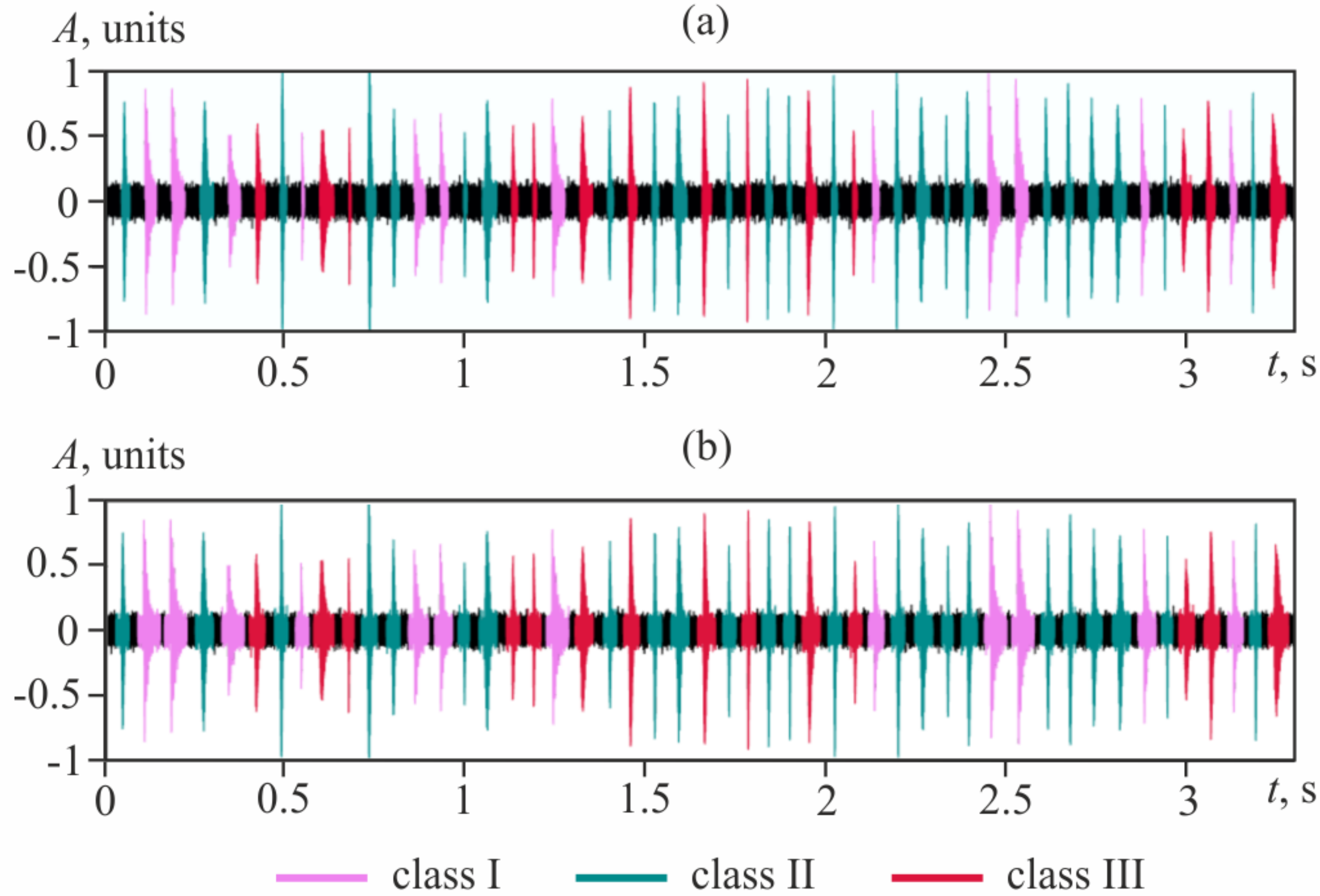

Fig. 10. Classification results: (*a*) – signal with overlapped white noise and initial structuring into classes; (*b*) – classification of $S_0 = 0.6$, $G_0 = 0.7$; three classes were defined.

6. Results

The following methods have been developed and applied for geophysical signal analysis:

- **Waveform reconstruction**
- **Pulse detection**
- **Time-frequency analysis method**
- **Waveform analysis method**

Thank you for your attention!

Overview of processing and analysis methods for pulse geophysical signals

O. Lukovenkova, Yu. Senkevich,
A. Solodchuk, A. Shcherbina

На тестовом сигнале:
Найдено 277781 импульса, из них отсеялись:
140871 - короткие
20024 - тихие
1007 - неправильной формы